Fully Soot sheet characterization in a Vertical Wall-Flame by Laser Induced Incandescence (LII)

VALENCIA Andres*, COPPALLE Alexis, TALBAUT Martine, GODARD Gilles, GOBIN Carole

Laboratory CORIA-UMR 6614, CNRS-Université et INSA de Rouen, France

Abstract

The aim of this work is to investigate the 2D slices though 3D soot-sheet into a turbulent non-premixed vertical-wall flame by using LII technique. Two studies are presented: A fully geometrical analysis and a velocity estimation of 2D soot-sheet. For the geometrical analysis, 2D spatially-resolved Laser Induced Incandescence (LII) has been performed. The surface, perimeter and major axis length of 2D soot-sheet have been determined. Evolution of soot-sheet dimensions within the height and the width in the flame are presented. It was found soot-sheet size and number increase within the height in the flame. For soot-sheet velocity, work is actually in progress about a new velocimetry methodology (Soot-Sheet Tracking Velocimetry). Principe, methodology and first results are presented.

1. Introduction

Soot particles play an important role in radiative heat transfer from flames. During their lifetime within a flame, soot is formed and reaches high temperatures. With a sufficient mass concentration, soot is the principal emitter of radiative heat, much than other molecular emitters formed during combustion [1]. This conditions are normally produced at large-scales flames, where radiation is the dominate mode of heat transfer [2] and the most contributor on fire growth and spread.

In turbulent flames, soot zones appear as non-homogeneous 3D sheet-like structures [3]. However, soot-sheet structures are strongly fluctuant in volume fraction f_v and dimension, so a statistical study is necessary. Xin and Gore [4] studied the distribution of soot of a methane and ethylene turbulent buoyant flame. They observed that the instantaneous peak of f_v is about an order of magnitude higher than the mean value, proving the high degree of fluctuation.

In order to study soot-sheet, two kinds of approach are usually used: soot-sheet dimension distribution [3] [5] and soot volume fraction distribution [4] [6] [7]. In the present work, only soot-sheet dimensions are studied.

For dimension distribution investigations, different techniques have been used. Miake-Lye et al [5] studied soot-sheet dimension in a large buoyant flame using a high speed camera and recording laser light scattered by soot. They determined that soot-sheet thickness and curvature are qualitatively constant toward the radial position of the flame. Qamar et al [3] used 2D laser Induced Incandescence (LII) to study soot-sheet dimension. They developed a method to study statistically and quantitatively soot-sheet dimension, based on an estimation of width and length. One of conclusions of this work is that the diminution of the soot-sheet number and of the soot-sheet dimensions is the principal fact of soot burnout, for precessing jet and simple jet flames.

Those investigations had an important impact on qualitative and quantitative analyze of soot-sheet structures in flames, their influence on soot production and burnout, and their fluctuant behavior. However, quantitative measurement of soot-sheet dimensions within a turbulent flame is relatively recent, and fully measurements of dimension properties (surface area, perimeter, major and minor axis length) of soot-sheets have not been reported.

Motived for that, the aims for this work are: i) characterize statistically soot-sheet dimension in a turbulent vertical-wall flame. Pdf's of the surface area, perimeter, and major axis length are calculated, ii) study the influence of the height in the flame on production and burnout of soot through statistical soot-sheet properties analysis. iii) Propose a methodology of image post-treatment adapted at 2D soot-sheet analysis. In addition, work in progress on the research of soot-sheet velocity measurements will be presented.

2. Experimental Setup

2.1. Vertical Burner. The flame is generated by a gaseous burner in a vertical configuration to obtain a wall fire configuration. The burner is a 20 x 40 cm bronze porous burner, fed with methane (0.243 x 10 g/s) and ethylene (0.512 g/s). To stabilize the flame, a steel wall cooled with water has been installed around the burner, and a gaseous line fed with methane (0.017 g/s)

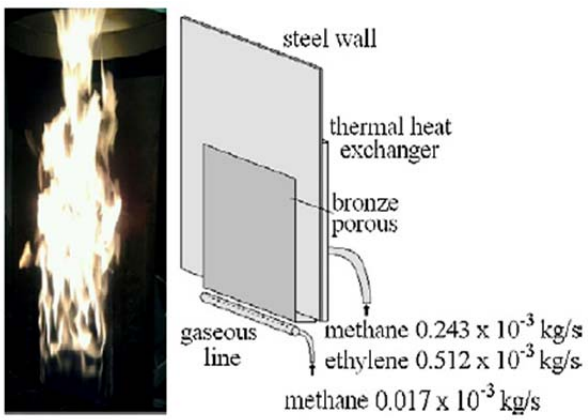

Fig 1. Porous vertical burner fed with methane and ethylene. A flame of 90 cm of height is generated.

*Corresponding author. valencia@coria.fr

has been installed at the bottom of the burner.

More details of the burner are described by [8] and [9].

2.2. LII Setup. The LII setup is shown in the figure 2. A laser Nd:Yag (Quantel Brio) at 532 nm (2ω) was used. This laser generates a pulse of ~10 ns with a 20 Hz repetition rate. As explained by D. Hebert et al [8], the second harmony was preferred due to the important energy density and more stable power output. Two lenses, a cylindrical with f = -10 cm and a spherical with f = 150 cm have been installed to generate a Gaussian laser sheet with ~3.8 cm of length and ~0.74 mm of width (FWHM). A mirror has been installed to direct vertically the laser sheet. The camera used to record the LII signal was an intensified CCD Princeton PIMAX 4:1024i, with 50 mm zoom lens. A study field of 14.5 cm of height and 4 cm of width, with a resolution of 145µm/pixel (1024x1024 pixels) has been chosen.

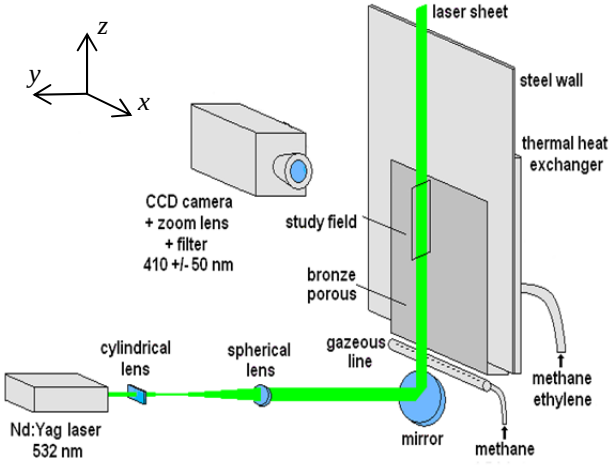

Fig 2. Experimental setup of LII measurements.

In order to avoid interference of PAH and light scattering by soot particles, the detection gate has been delayed 30 ns relative to the laser pulse [10] [4]. Also a pass band filter centered at 410±50 nm has been installed on the camera in order to eliminate undesired signals and to enhance the signal-to-noise ratio. The width of the gate has been setup on 70 ns. Choice of laser fluence is discussed at section 4.

For Soot-Sheet Laser Velocimetry (section 6) a second similar laser was installed in order to have two aligned beams. The two lasers were synchronized in order to have 400 µs between the two pulses. The module DIF (Double Image Feature) of the camera has been activated, allowing to record two full-resolution LII images consecutively. Each gate has been set at 70 ns of gate width and 30 ns of gate delay in relation with the two laser pulses.

3. Methodology

Dimension properties of soot-sheet were measured. Due to the complexity and irregularity of soot-sheet, 3 dimension properties were chosen in order to characterize as well as possible soot-sheets: Surface, perimeter and major axis length (in z direction). To characterize the shape of soot-sheet, alpha factor was also calculated (section 5). Considering the number of soot-sheets present by experiment (~2500 for 1000 LII-images), the development of an automate method was necessary.

At first, a digital filter is applied for each image, the non-linear operator "median filter". The goal is to enhance the signal-to-noise ratio at the edge of the soot-sheet; this facilitates the edge detection and helps to simplify soot-sheet segmentation. Thresholding is next applied to binarise the LII image.

It's important to note the higher the threshold value, the lower soot-sheet dimensions, and consequently special attention should be paid on the choice of the binarising threshold. In their investigation, Qamar et al [3] used a threshold in which the gradient of local f_v increases significantly and the loss of the sheet-like structure is minimal. In this work, the optimal threshold is a trade-off between the level of change in soot-sheet dimensions and the signal-to-noise ratio. For all the LII images, a threshold of 2% of the maximal signal detected during a series of measures is used. The influence of the threshold value on soot-sheet dimensions determination will be study in further works.

Then, a morphological operator "opening" is after applied to eliminate small and isolated soot-sheets [3]. In average, a LII image contains 20 times more of small and isolate sheets than coherent soot-sheet-like structures. In this work, these structures are not considering as soot-sheet but as noise, so they are not taken into account. Definition of the soot-sheet edge and image treatment is achieved with the opening operator.

Determination of soot-sheet dimensions start by contour detection. A classical Freeman 4-directional chain code (FFDCC) [11] was used. Once contour is detected, dimensions properties (surface area, perimeter, length and centroïde) and shape properties (alpha. Definitions at section 5) are determined.

4. Laser Fluence Dependence

LII signal is dependent on laser fluence. While laser fluence increases, soot particle temperature rapidly rises until vaporization point. If fluence keeps rising, sublimation and soot particle mass loss will cause a decrease in LII signal. In the same way, LII signal is also dependent on laser beam spatial profile. For one dimensional Gaussian sheet beam profile, LII signal loss from sublimation is compensated by a gain in LII signal in the wings of the laser sheet, where sublimation have not been reached. This compensation generates a 'plateau' region where LII signal is less (or not) dependent of laser fluence [12] [10]. Laser energy fluences at plateau region are preferred in order to avoid uncertainties in LII measurements produced by shot-to-shot laser energy changes.

However, for soot-sheet dimensions measurements, both effects (LII signal decrease by sublimation and LII signal increase in the wings of the laser sheet) could influence differently the size and the shape of soot-sheets. For example, the gain in LII signal in the wings of the laser beam through the *y* and *x* axis will generate an increase on the effective LII probe volume, so on the calculated soot-sheet size.

The figure 3a shows the fluence dependence of averaged LII signal, calculated as the average of the integrated LII signal in an interest zone of 4 cm and 3 cm in *y* and *z* axes respectively. The fluence dependence of the LII signal peak is also shown, calculated as the average of the maximal LII signals recorded in each LII images. Peak of LII signal is expected to be less dependent on laser beam shape i.e. more dependent on sublimation than average LII signal. For each value of fluence, 500 LII images (~ 1700 soot-sheet) were studied.

For the two fluence curve, plateau LII takes place after 0.23 J/cm². This value is consistent with typical values available in literature [10]. However it was found that the plateau region is clearer for the peak of LII signal than for averaged i.e. peak-LII signal is less dependent of fluence than spatial-averaged signal after plateau region reached. It suggests that the gain on emitted LII signal by increasing the effective LII probe volume makes the gated LII signal more dependent of laser fluence.

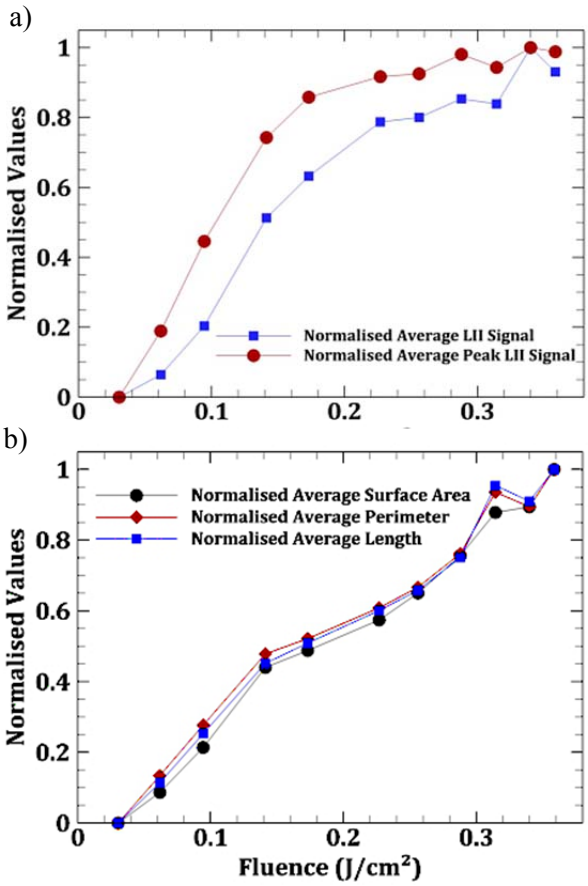

Fig 3. Normalized fluence curves for a) LII Signal (peak and spatial-average), b) Soot-sheet dimensions (Surface area, perimeter and length). For each value of fluence, 500 images (~ 1700 soot-sheet) were analyzed. Each profile was normalized to the unity with the maximum value of each curve

This effect is more significant for soot-sheet dimensions. The figure 3b shows the fluence dependence of average soot-sheet dimensions (surface area, perimeter and length). Each point is the average of the soot-sheet dimensions detected in 500 LII images (same data than for LII signal). It was found that soot-sheet dimensions continually increase without stabilization, so the plateau region wasn't found. It means that soot-sheet dimensions depend on laser fluence, and not specific fluence value could be chosen to avoid it. In this work, a laser fluence of 0.23 J/cm² has been chosen to make sure that LII signal is at the plateau region. However, more studies should be carried out concerning soot-sheet dimensions dependence on fluence.

5. Results and discussions

5.1. Soot-Sheet Dimensions in function of the height in the flame. Determination of soot-sheet dimensions has been performed along the burner vertical axis from 15.5 cm to 42 cm. Three series of measures of 1000 images were performed, from 15.5 cm to 30 cm, from 20 cm to 34.5 cm and from 27.5 to 42 cm. The figure 4 shows the probability density distribution (pdf) of soot-sheet dimension surface area, perimeter and length, at the 3 vertical positions. More than 2000 soot-sheet by series of measure were treated.

Perimeters from 1 to 80 cm were measured. Soot-sheets with perimeter greater than 40 cm were found to have large dimensions with multiple branches. However, most of soot-sheets are included between 1 cm and 20 cm, with a lot of soot-sheet with small dimensions. The Pdf's of surface area are similar. Surface areas from 0.3 cm² to 33 cm² have been detected. Soot-sheets with surfaces greater than 9 cm² have complex and irregular geometries. For the lengths, values from 0.1 cm to 10 cm have been detected.

The maximal surface areas and perimeters around 32 cm² and 80 cm respectively have been measured at the top of the burner, while at the bottom around 22 cm² and 52 cm. This shows that soot-sheet dimensions increase with the height in the flame. Two phenomena could explain this change in soot-sheet dimension. First, wall-flames are buoyancy-driven phenomena, so soot-sheet created at the bottom move up from position I to III. During this transport process, soot-sheets are within the reaction zone and production of soot could happen at the interface, leading a growth on soot-sheet dimensions. Nevertheless, transports phenomena on horizontal axis are also present i.e. soot-sheet also move from rich to poor reactions zones. At poor zones, important amounts of air could induce dilutions effects

on soot-sheet, so growth on soot-sheet dimensions and reduction of local soot concentration.

In addition, the increase of the soot-sheet number with height in the flame has been also observed: 2139, 2309 and 2848 soot-sheets respectively for the 3 studied heights. These observations suggest that important amounts of soot are vertically transported. However, the growth of the soot-sheet number could be also explained by the detachment of those with important dimensions. While soot-sheet going up in the flame, turbulence of flame induces important changes on it shapes, starting by the deforming (ex. multiple branches soot-sheets) and finish by detachment.

In order to study changes in the shape of soot-sheet, factor alpha was studied. Alpha is a measure of the level of stretch of soot-sheet. Alpha is defined as $\propto = \frac{Major\ axis\ lenght}{Minor\ axis\ lenght}$. Typical values between 1.01 and 40 were found. Soot-sheet with $\propto < 3$ have found to be very smalls. Soot-sheets with $3 < \propto < 10$ have found to be mono branches, homogenous. Figure 5 shows typical soot-sheet shapes, soot-sheet a) and c) have $\propto_a = 7$ and $\propto_c = 5$ respectably.

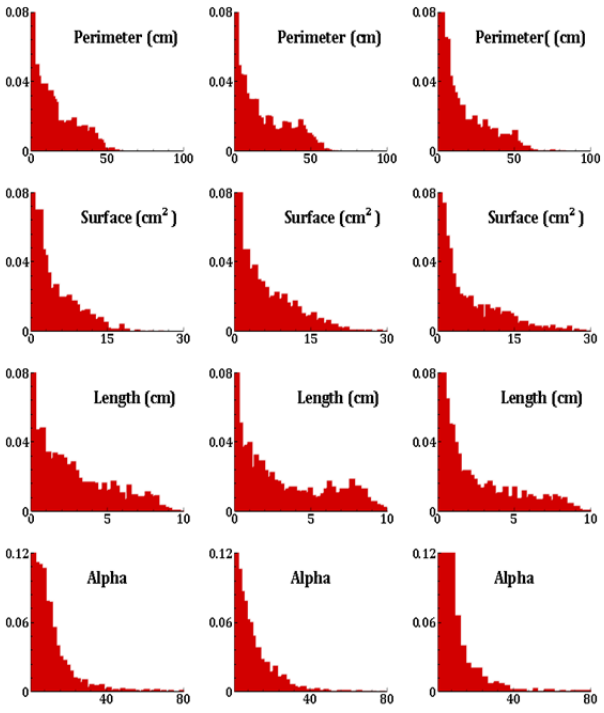

Fig 4. PDF of soot-sheet dimensions properties for two for three vertical position: i) left column: from 15.5 cm to 30 cm, ii) center column: from 20 cm to 34.5 cm and iii) right column: from 27.5 to 42 cm.

Exceeded $\propto = 10$, stretch in soot-sheet starts to be important and higher dimensions are found. In figure 5, d) is a typical stretched soot-sheet whit $\propto_d = 23$. Vertical direction is always privileged. Multi branches soot-sheet have also values of alpha higher than 10. At figure 5, b) is a complex and multi branches soot-sheet with $\propto_b = 15$.

Alpha factor has been studied at the three vertical positions. Not important change in histograms has been observed.

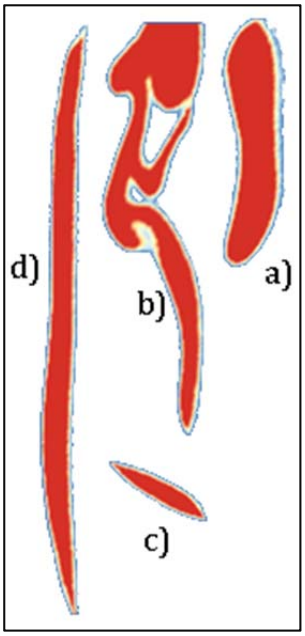

Fig 5. Example of soot-sheet with different values of $\propto$ a) $\propto = 7$, b) $\propto = 15$, c) $\propto = 5$, d)$\propto = 23$

5.2. Soot-sheet Dimensions in function of y-axis

In order to investigate the evolution of soot-sheet dimension through the width of the flame, a study 1D has been carried out thought y-direction. The figure 6 shows the 2309 soot-sheet detected and treated from 20 cm to 34.5 cm from the bottom of the burner. Each point represents the surface area (as representation of soot-sheet dimensions) of each soot-sheet in function of the transversal position (*y*-axis) of each soot-sheet centroïde. The averaged normalized LII-signal at the middle of the field (as representation of soot volume fraction, averaged with 1000 LII images) is also showed.

Soot-sheets through y axis have been found to evolve in 4 different regions. First, the near-wall region starts from the burner-wall (y = 0) to y = 0.6 cm. This is characterized by low soot concentration, and low number and dimension of soot-sheets. Soot-production region, between y = 0.6 cm and y =1.6 cm is characterized by an important increase of soot concentration, and also of soot-sheet number and dimensions. Note that the peak of volume fraction is reached early, particularly because of the increase of the soot-sheet number. Consequently, in this region, the soot concentration is controlled by the number of soot-sheet more than the dimension of soot-sheet. It's important to note that after having reached the peak of soot concentration near of 1 cm, there is a plateau region where soot concentration is constant. This is due

to a trade-off between soot-sheet dimensions and soot-sheet number, while soot-sheet dimensions increases, soot-sheet number decrease along the y-axis.

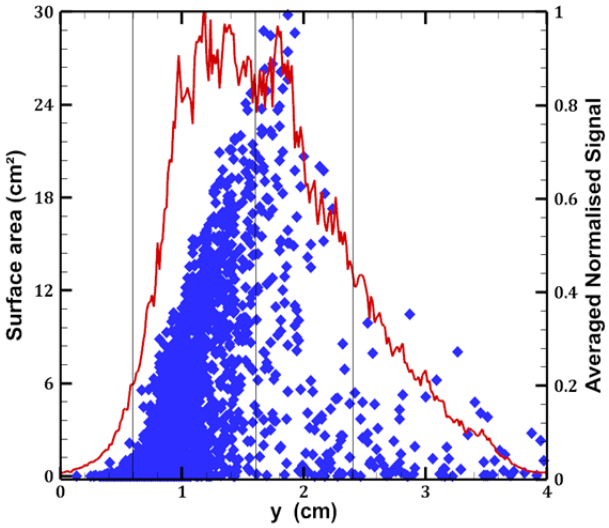

Fig 6. Soot-sheet surface area (blue) and averaged normalized LII signal (red) in function of the *y* axis.

The fully-developed dimensions region is located between 1.6 cm and 2.2 cm. It's characterized by decrease of soot-sheet number (mainly smalls), the reach of soot-sheet dimension peak and the beginning of soot concentration decrease. Note that the soot-sheets of biggest dimensions are located in the plateau region of soot peak concentration, even if the number of soot-sheet is considerably smaller than at soot-production region. It suggests that this region is basically controlled by the soot dimensions. After 2.2 cm the soot-burnout region is located. In this region, it is found a decrease of soot concentration, soot-sheet number and soot-sheet dimensions.

6. Soot-sheet Tracking Velocimetry

6.1. Principle. A new technique of velocity measurements of soot-sheet is being developed. In this work principle, progress and first results are presented.

Soot-sheet Tracking Velocimetry is a LII-based technique, in which two consecutive aligned laser shots excite soot within the flame. The experimental setup is described at section 2. Two 2D soot fields (LII images) are obtained at the same position in the flame. After post-treatment process described at section 3, two binarised 2D soot-sheet field are obtained.

In order to calculate the displacement field, a correlation method based on soot-sheet dimensions is used. The principle is to calculate dimensions properties of each soot-sheet detected at the first soot-sheet field, correlates with the consecutive soot-sheet field and calculate displacement field by subtracting centroïde coordinates of each couple of correlated soot-sheet.

6.2. Comparison Filters. Each soot-sheet of the first image is compared with each soot-sheet of the consecutive image. Three kind of comparison are realized in order to do correlation i.e. to determine if a soot-sheet detected in the first soot-sheet field is also detected in the second soot-sheet field. Each comparison is named 'filter' thereafter. The filters are applied one after the other

Soot-sheet shape filter is the first step. The goal is to do a first comparison between soot-sheets of the two consecutive images, and segregate soot-sheet with complex geometries, in order to a) reduce uncertainties linked to the calculation and correlation of centroids (ex. soot-sheet with centroïde located out of contour) b) limit inhomogeneous displacement of soot-sheet contour (ex. multi-branches soot-sheet) c) Avoid soot-sheet that rotates. To do that, two shape factors are calculated, alpha and beta. Beta is defined as $\beta = \frac{Soot\ sheet\ surface}{Feret\ rectangle\ surface}$, where the *Feret rectangle surface* is the surface of the smallest rectangle enclosing the soot-sheet, with its sides at *z* and *y* axis direction.

Soot-sheet-dimensions-filter is the second filter. Surface area, perimeter and length of soot-sheet of two consecutive images are compared. Only soot-sheets with surface areas lower than 4 cm² are accepted. This is necessary because, if a large soot-sheet undergoes deformations, the centroïde-based velocity calculation might not represent the velocity of the entire soot-sheet. Finally, the third filter soot-sheet-coordinate-filter is applied. The y and z coordinates of the centroïde of soot-sheets are compared with a maximal displacement value δ, in order to avoid ambiguity when two couples of correlated soot-sheet have similar characteristics (surface area, perimeter, alpha, etc.).

A flexibility factor f is defined in order to set the precision of the correlation. For example, if the property $p(s_1)$ of soot-sheet s_1 of the first image is compared with the properties $p(o_2)$ of the soot-sheet o_2 of the consecutive image, $s_1 = o_2$ if

$$(1-f) * p(o_2) < p(s_1) < (1+f) * p(o_2)$$

6.3. Soot-sheet Velocity Calculation. After applied the three filters, only ~17% of soot-sheet are selected to realize velocity calculation (for $f = 0.15$). If soot–sheets s_1 and $o_2$are identical, velocity is defined as:

$$\overrightarrow{v(s_1)} = \frac{\overrightarrow{O(o_2)} - \overrightarrow{O(s_1)}}{\Delta t_{LII}}$$

Where the vector $\vec{O}$ is the coordinate of soot-sheet centroids and Δt_{LII} is the time between the two camera gates. Velocity is calculated for correlated soot-sheets.

6.4. First Results. The figure 7 shows the distribution of soot-sheet velocities measured for *y* and *z* direction. A flexibility factor $f = 0.15$ was used and 44 pairs of soot-sheet were correlated. The experiment was carried out between 15.5 and 30 cm in *z*-direction. 1000 pairs of LII images was taken. $\Delta t_{LII} = 400\ \mu s$.

For vertical velocities values from -200 cm/s to 200 cm/s have been found. With a Gaussian fit, the distribution is centered at 57 cm/s. Horizontal velocities

are found to be lower, with values between -100 cm/s and 150 cm/s centered at around 40 cm/s.

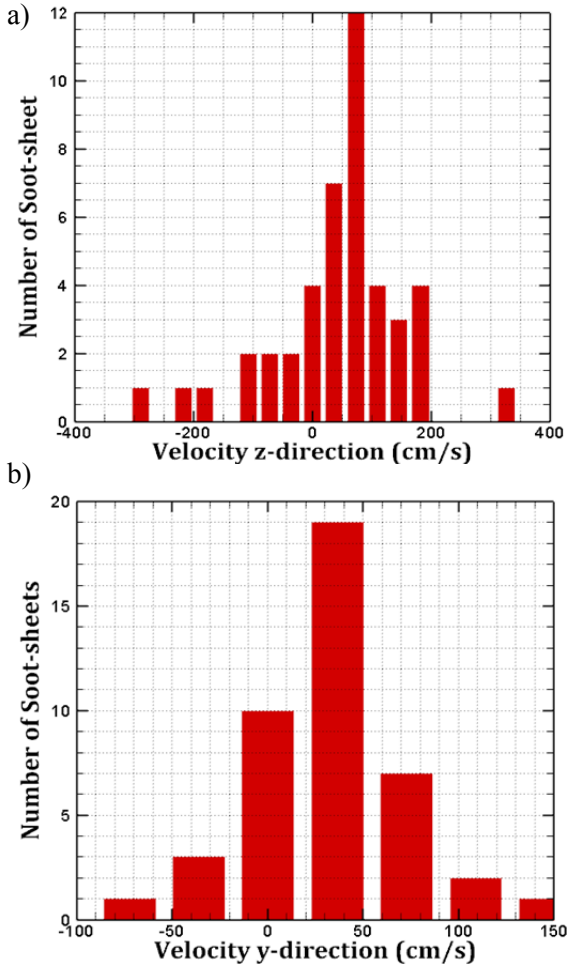

Fig 7. Soot-sheet velocity Distribution a) horizontal velocity component (y direction) b) vertical velocity component (z direction). 1000 pairs of LII-Image analyzed (419 pairs of soot-sheet). Study field from 15.5 cm to 30 cm (axe z). f = 0.15. $\Delta t_{LII} = 400\ \mu s$.

Negative velocities values have been also observed. It could be related to i) the high level of turbulence in the flame: soot-sheets located into vortex, ii) Velocity measurements of soot-sheet with sections cut out by the image boundary, iii) 3D soot-sheet displacements in x-direction. All this phenomena will be studied in order to quantify their effect on soot-sheet velocity measurements. In addition, further soot-sheet velocity analysis will be carried out with more data (soot-sheet) in order to enhance the quality of the results.

7. Conclusions

of LII image post-treatment has been realized to analyze 2D soot-sheet, allowing the determination of soot-sheet dimensions (surface area, perimeter, maximal length). Soot-sheet with surface areas and perimeters greater than 40 cm and 9 cm² respectively have been found to be complex and with irregular geometries. Soot-sheet shape has been studied by determining $\propto$ factor. Soot-sheet with $\propto < 15$ are homogenous and mono-branches, exceed this value soot-sheet begins to have multi-branches and irregulars.

Soot-sheet dimensions have been determined along the burner vertical axis from 15.5 cm to 42 cm. The PDFs of soot sheet surface and number showed that soot-dimensions and number increase with the height in the flame, suggesting that important amounts of soot are vertically transported.

Soot-sheet dimensions along the horizontal direction have been studied. They are found to evolve in 4 different regions: i) the near-wall region characterized by low soot concentration, low soot-sheets number and soot-sheet dimensions, ii) Soot-production region, characterized by important increase of soot concentration, soot-sheet number and soot-sheet dimensions, iii) The fully-developed dimensions region, characterized by decrease of soot-sheet number (mainly smalls), the reach of soot-sheet dimension peak and the beginning of soot concentration decrease, iv) soot-burnout region where soot concentration, soot-sheet dimensions and soot-sheet number decrease.

Finally, progress in Soot-sheet Tracking Velocimetry technique has been presented. The principle and methodology was detailed. The soot-sheet velocity distributions showed velocities between -2 m/s to 2 m/s in z-direction, and between -1 m/s and 1.5 m/s in y-direction. Further works will be focused on the influence of flame turbulence and 3D soot-sheet displacement in x–direction on soot-sheet velocity.

References

[1] J. Fenghui, Fire Safety Journal 30 (1998) 383-395.
[2] J. Fenghui, J.L. de Ris, M.M. Khan, Fire Safety journal 44 (2009) 106-112
[3] N.H. Qamar, G.J. Nathan, Z.T.Alwahabi, Combustion and Flame 158 (2011) 2458-2464.
[4] Y. Xin and J.P. Gore. Proceedings of the Combustion Institute 30 (2005) 719–726.
[5] R.C. Miake-Lye, S.J Toner, Combustion and Flame 67 (1987) 9-26.
[6] N.H. Qamar, Z.T. Alwahabi, Q.N. Chan, G.J. Nathan, D. Roekaerts, K.D. King, Combustion and Flame 156 (2009) 1339-1347.
[7] N.H. Qamar, G.J. Nathan, Z.T. Alwahabi, K.D. King, Proceedings of the Combustion Institute 30 (2005) 1493–1500.
[8] D. Hebert, A. Coppalle, M. Talbaut, Proceedings of the Combustion Institue 34 (2013) 2575-2582.
[9] G. Bertin, J. Most, M. Coutin. Fire safety journal 37 (2002) 615-630.
[10] C. Schulz, B.F. Kock, M. Hofmann, H. Michelsen, S. Will, B. Bougie, R. Suntz, G. Smallwood, Appl. Phy. B 83 (2006) 333-354.
[11] H.Fremman, IEE Transactions on Electronics 10 (1961) 260-268.
[12] P. Desgroux, X. Mercier, K.A. Thomson, Proceedings of the Combustion Institute 34(2013) 1713-1738.